Vessel Width Estimation via Convolutional Regression

Rui-Qi Li[1,2], Gui-Bin Bian[1,2], Xiao-Hu Zhou[1,2], Xiaoliang Xie[1,2], Zhen-Liang Ni[1,2], Yan-Jie Zhou[1,2], Yuhan Wang[1], and Zengguang Hou[1,2,3,4](✉)

[1] State Key Laboratory of Management and Control for Complex Systems, Institute of Automation, Chinese Academy of Sciences, Beijing 100190, China
zengguang.hou@ia.ac.cn

[2] School of Artificial Intelligence, University of Chinese Academy of Sciences, Beijing 100049, China

[3] Center for Excellence in Brain Science and Technology, CAS, Beijing 100190, China

[4] CAS-MUST Joint Laboratory of Intelligence Science and Technology, Institute of Systems Engineering, Macau University of Science and Technology, Macau 999078, China

Abstract. Vessel width estimation has a wide range of applications in disease diagnosis and treatment. In this paper, vessel width estimation is cast as a regression problem, and a novel Convolutional Neural Network (CNN) based method is proposed for vessel width estimation. In our CNN-based method, the idea of divide-and-conquer is introduced to solve the challenge of imbalanced training samples. Besides, in order to solve the shortage of training samples required by CNN, a vessel width label generation method is proposed to generate width labels from vessel segmentation labels. In the experiments, we apply our vessel width label generation method and CNN-based width estimation method to two tasks which are retinal vessel width estimation and coronary artery width estimation. Experimental results show that our width label generation method can generate sufficiently realistic width labels using accurate segmentation labels. Also, our CNN-based method can solve the challenge of imbalanced training samples, achieving state-of-the-art performance with less inference time.

Keywords: Vessel · Width estimation · Deep learning

1 Introduction

The vessel width estimation plays a weighty role in both disease diagnosis and clinical treatment. For retinal vessel, studies have shown that a decreased ratio of arterial to venous retinal vessel width forms an independent risk factor for stroke, myocardial infarct as well as eye disease [1]. For coronary artery, during the implementation of percutaneous coronary intervention, surgeons need to measure the width of the coronary artery to determine the type of the stent. Therefore, vessel width estimation has a wide application prospect.

M. de Bruijne et al. (Eds.): MICCAI 2021, LNCS 12906, pp. 600–610, 2021.
https://doi.org/10.1007/978-3-030-87231-1_58

Existing vessel width estimation algorithms fall into two categories: semi-automatic [2,3,10] and fully automatic [4–9,11]. The semi-automatic algorithms require the user to nominate the profile of the vessel, and then locate the positions of two vessel edges by analyzing the changes of the pixel intensity on the profile. The vessel width on this profile is the distance of two vessel edges. Since the user is required to nominate the profile, the quality of the estimation result largely depends on the accuracy of the profile given by the user. Instead of requiring the user to nominate a profile, the fully automatic algorithms can estimate the widths of all the vessel segments in the image. Fully automatic algorithms first segment all vessels, then extract the centerline of the segmented vessels and compute the profiles of all vessels. Finally, vessel widths are calculated by a semi-automatic method with the calculated profiles.

Semi-automatic algorithms require the user to nominate the vessel profile and are not intelligent. Although automatic algorithms are intelligent, all the operations in automatic algorithms (extracting the centerline, calculating the vessel profiles and predicting the width of all the profiles) require repeated processing of all the image pixels, resulting in the processing time of an image requiring tens of seconds or even minutes. Therefore, an automatic and fast vessel width estimation algorithm needs to be proposed.

Up to now, many methods based on Convolutional Neural Network (CNN) have been used in many fields of medical image processing, but as far as we know, the CNN-based method has not been applied to the vessel width estimation task. The main reason is the lack of datasets that can be used for training. Besides, how to use CNNs to predict the vessel widths is also a problem to be solved. In this paper, we address the above difficulties by proposing a vessel width label generation method and a novel CNN-based vessel width estimation method. Compared with the existing automatic algorithms, our CNN-based method can achieve the same or even better results in precision, and far exceeds the existing methods in speed.

Our contributions are as follow: (1) The width estimation problem is transformed into a pixel-level width regression problem, which brings a new idea to solve this problem. (2) To address the lack of width labels for training, a vessel width label generation method is proposed. (3) A CNN-based method for automatic vessel width estimation is proposed, which can solve the uneven width distribution in training samples. To the best of our knowledge, our method is the first work that uses a deep learning model for vessel width estimation.

2 Method

2.1 Vessel Width Label Generation Method

To address the lack of width labels for training, a method that generates vessel width labels using the vessel segmentation labels is proposed. This method has similar procedure with existing automatic width estimation algorithms. However, since the difference of algorithm objective, our method has different processing in some steps compared with existing width estimation algorithms. Here, taking the coronary artery as an example, we will describe our method. We only detail the special parts of our method, and briefly cover the parts that are the same as the existing width estimation algorithms. The processing steps are as follow:

(1) Extract the coronary artery centerline in the segmentation labels. The thinning algorithm we use is the method proposed in [12].
(2) Remove the intersection points and bifurcation points in the coronary artery's centerline. After these points are removed, the coronary artery tree is cut into artery segments, as shown in Fig. 1(c). In our implementation, artery segments with length less than 10 pixels will be then removed.
(3) Calculate the profile of each pixel on the remaining centerline. Here, we apply the method proposed in [8], that is, using several adjacent centerline pixels on both sides of the target pixel and applying principal component analysis on these pixels. A profile result is shown as the blue line in Fig. 1(d).
(4) Find two artery edge points on each profile and calculate the artery width. Since the accurate segmentation labels have been given, the boundaries between vessel and non-vessel pixels in segmentation labels are the edges of the artery. Therefore, the two edge points are the intersections of the profile and two segmentation boundaries. In our implementation, we proceed from the centerline pixel (red pixel in Fig. 1(d)) along the profile to both sides at a certain step size (0.1 pixel we use), and calculate the intensity of the current coordinate using bilinear interpolation at each step. When the intensity value is less than 0.5, the current coordinate is the edge point. As shown in Fig. 1(d), two yellow cross points are the two edge points calculated this way. The artery width on this profile is the distance between two edge points.
(5) Generate the final labels. For training and for test, the generated labels are different. For test, two edge points' coordinates are regarded as a test sample, just like REVIEW dataset [13]. For training, to train a pixel-level width estimation algorithm, we assign the width value to all the pixels that belong to both the profile and the coronary artery, as shown in Fig. 1(e). There are two purposes to do this. First and most intuitively, this way can enlarge training samples, especially the training samples of thick vessels. Second, in application, we hope to obtain uniform width estimation results

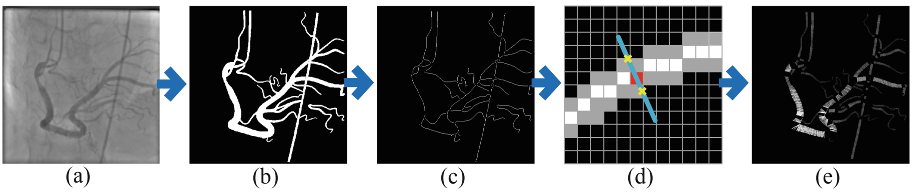

Fig. 1. (a) The raw image. (b) Corresponding segmentation label. (c) Coronary artery centerline without intersection and bifurcation points. (d) White pixels are centerline pixels, gray pixels are artery pixels. Blue line is the calculated profile of red pixel, and yellow points are two edge points on the profile. (e) Generated labels for training. (Color figure online)

regardless of which pixel is selected among all the pixels belonging to the same profile. In this generating way, many pixels have no width values, and these pixels will not be used in training. Besides, there will be pixels that belong to multiple profiles and have multiple width values. In this case, we will assign the mean width value to these pixels.

It is worth noting that the labels generated by this method inevitably have very few error labels. For deep learning methods, very few error training labels can not affect the final result. However, for the test labels, you must manually check and eliminate all error labels.

2.2 Vessel Width Estimation Network

In this paper, vessel width estimation is cast as a pixel-level width regression problem, which means to predict a width value for each image pixel, and a CNN-based method is proposed to regress the pixel-level width by extracting the local image features. The vessel width can range from one pixel to dozens of pixels in the images, and the width distribution is often uneven. In general, thin vessels make up the majority of vessels, which will cause the width estimation algorithms to pay too much attention to thin vessels instead of thick vessels. However, from the point of applications, it is usually the thick vessels that need to be measured, while the width of the thin vessels is not important. Therefore, the imbalanced distribution is the main challenge in vessel width regression.

Inspired by the divide-and-conquer idea used in other numerical regressions [14,15], we partition the entire width range into many sub-ranges, and train a local regressor for each sub-range. Each local regressor only uses pixels whose width label belongs to its own sub-range in training to ensure its good performance in its sub-range, regardless of its performance in other sub-ranges. At the same time, a classifier is trained taking each local regressor as a category. The classifier is used for selecting appropriate regressors for different pixels by judging their width sub-ranges. The classifier is trained using the one-hot labels. The advantages of our method include: 1. In each sub-range, the distribution of vessel widths is relatively even. Therefore, the challenge of imbalanced distribution has been addressed. 2. With the partition of the range, the difficulty of each regression task is reduced, which helps to obtain finer regression results.

To implement the regressor and classifier, a network is proposed in Fig. 2. This network can actually be viewed as an U-net [16] with two decoding branches. Compared with U-net, we reduce the depth of the network, and replace the deconvolutional layer with bilinear upsampling layer to reduce the model parameters. As shown in Fig. 2, both the regression branch and the classification branch output the results with the size of $\mathrm{H} \times \mathrm{W} \times \mathrm{N}$. N is the number of sub-ranges, also the number of local regressors. Each output channel of the regression branch represents the estimated widths of each local regressor for all pixels. For each pixel, N local regressors output N width predictions ($1 \times 1 \times \mathrm{N}$). The classification branch outputs the probability ($1 \times 1 \times \mathrm{N}$) that each pixel belongs to N

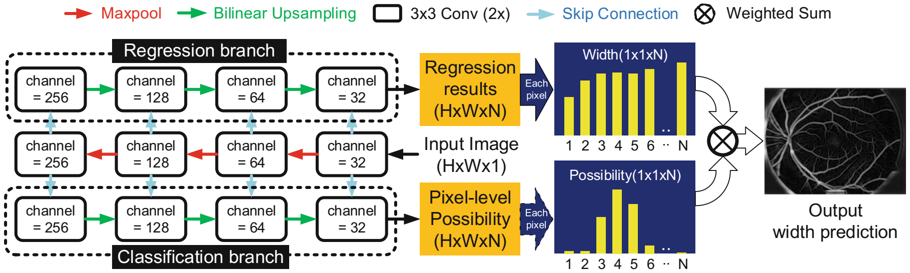

Fig. 2. Schematic diagram of our CNN-based method. N is the number of sub-ranges.

regressors. Instead of using the predicted width of the local regressor with maximum probability, the output width of each pixel is the weighted sum of the predicted widths of all regressors taking the probability as weights. The use of weighted sum is beneficial to obtain smoother width estimation results.

For the loss function, mean-square error loss is used for the regression, and softmax cross-entropy loss is utilized for the classification.

$$\begin{aligned} Loss &= \lambda L_{reg} + L_{cls} \\ &= \frac{\sum_{i=1}^{P}[\lambda(W(i) - W^*(i))^2 - \sum_{j=1}^{N} p(j)log\ q(j)]\delta(v_i = 1)}{\sum_{i=1}^{P}\delta(v_i = 1)} \end{aligned} \tag{1}$$

where P is the number of pixels, N is the number of sub-ranges. v_i is the trainable flag for pixels, and only the pixels have width labels are used in training. W and W^* are the predict width and ground-truth width respectively. $q(j)$ and $p(j)$ are the output and ground-truth probabilities, λ is the weight set for L_{reg}.

3 Dataset

3.1 Retinal Vessel Dataset for Width Estimation

There is an open dataset for evaluation of the width estimation task of retinal vessel: REVIEW [13]. The REVIEW dataset includes four image sets and we only use three of them those are challenging (KPIS is not used since it only contains 3 vessel segments): (1) High Resolution Image Set (HRIS); (2) Vascular Disease Image Set (VDIS); (3) Central Light Reflex Image Set (CLRIS). These image sets include 14 images with 190 vessel segments, and contain 4902 manually marked profiles in total. These profiles are marked by three observers, with the mean value used as the ground-truth width. Since the dataset was established in 2008, before the boost of deep learning methods, this dataset is aimed at the unsupervised retinal vessel width estimation methods, and only contains the test samples. Two samples are shown in Fig. 3(d–e).

In order to obtain training samples for our CNN-based method, we use the proposed width label generation method to generate. The utilized segmentation

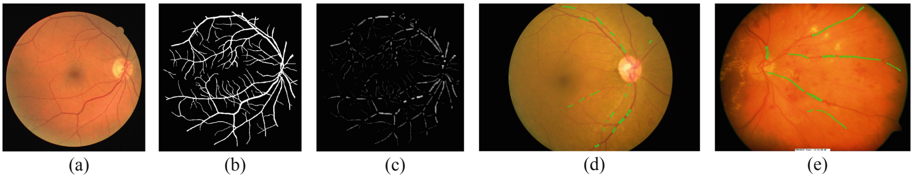

Fig. 3. (a) A sample in DRIVE dataset. (b) Segmentation label of (a). (c) Generated training label of (a). (d–e) Two samples in REVIEW dataset. The green part is the vessel segments with manually marked profiles. (Color figure online)

dataset is the most commonly used dataset: DRIVE [17]. DRIVE dataset contains a total of 40 images with precision pixel-level segmentation annotations, of which 20 images for training and 20 images for test. Each image has a resolution of 565×584. An image sample is shown in Fig. 3(a). The segmentation label and generated vessel width labels are shown in Fig. 3(b–c). Due to the existing of REVIEW (test samples), all 40 images of DRIVE dataset are used as the training samples of our proposed CNN-based method.

3.2 Coronary Artery Dataset for Width Estimation

Unlike retinal vessels, there is no public width estimation dataset for coronary arteries, or even a public segmentation dataset. Therefore, a coronary artery segmentation dataset established by us is used to generate the required training and test samples. Our segmentation dataset includes 745 images selected from 25 independent Digital Substraction Angiography (DSA) continuous sequences. Among them, 568 images from 13 DSA sequences are used as the training set, and 177 images from 12 DSA sequences are used as the test set. The DSA sequences are generated by Siemens Artis zee III ceiling, and are based on a flat panel detector. Each image has a resolution of 512×512. Using our proposed width label generation method, training samples and test samples for width estimation will be generated by the training samples and test samples of segmentation dataset respectively.

4 Experiment

4.1 Retinal Vessel Width Estimation

Our CNN-based method is compared with existing methods on the REVIEW dataset to verify the superiority of our CNN-based width estimation method and the effectiveness of the width label generation method.

Implementation Details: Similar to other methods [6,8], only the green channel of the retinal image is used as input, since the green channel shows the highest contrast between the blood vessels and background. Since the training set and the test set are from two independent datasets with a large scale difference, in order to ensure the consistency of vessel width distributions of the two sets, the resolutions of all images should be unified. The resolution of the DRIVE images is doubled to 1130×1168. For the REVIEW dataset, the images of HDIS are resized to 1792×1232, the images of CLRIS are resized to 1440×960, and the images of VDIS remain unchanged (1360×1024).

Due to the limited training data, we adopt a commonly used trick in retinal vessel segmentation: image cropping. During the training, the image patches of 288×288 are randomly cropped from the training images as the network input. Except random image cropping, random flip, random grayscale adjustment between -20 to 20, and random contrast ratio between 0.8 to 1.2 are also adopted for image augmentation. The retinal vessel width ranges from 0 to 20 pixels. We set the sub-range to be 4 (5 sub-ranges in all). λ in loss function is 5. The network is implemented using Tensorflow 1.10. For optimization, Adam optimizer [18] is applied with the batch size of 4. We use an initial learning rate of 0.0005, and the initial learning rate is multiplied by 0.8 every 1000 steps to avoid overfitting. Training takes about 3 h on an NVIDIA Titan XP for 2000 epochs.

Metric: Since REVIEW dataset is used for evaluation, the evaluation metrics designed by REVIEW dataset is also used. We report the success rate (SR) and the standard deviation of the width error (σ_E) as evaluation metrics. The success rate is the percentage of the test samples that the algorithm returns a meaningful width value. The σ_E is the metric proposed by the authors of REVIEW dataset. They argue that σ_E is more suitable to evaluate the performance of the width estimation algorithm, while the mean width error is incompetent in evaluation.

For our CNN-based method, these metrics are calculated in the following way: Firstly, since REVIEW dataset provides two edge points on the profiles, the center point coordinates and corresponding ground-truth vessel widths are calculated. Secondly, since CNN-based method will predict a width value for all pixels, the width corresponding to center point coordinate is the predicted width. Since the coordinates are usually not integers, bilinear interpolation is used to get the width predictions. Finally, the success rate and σ_E are calculated. Since each center point must have a return value, the value greater than zero is regarded as a meaningful measurement to calculate the success rate.

Experimental Results: Our CNN-based method is compared with some fully automatic and semi-automatic methods, including: HHFW, 1-D gaussian, 2-D gaussian, ESP, graph-based method, 3D model. The results are shown in Table 1. We can see that all success rates of our method are 100%. In terms of the σ_E, our method achieves state-of-the-art results on two of three sets: CLRIS and HRIS. It is worth noting that these results are obtained when the training data and the test data are from different datasets. We believe that the result can be better if the training data and the test data come from the same dataset. In addition, the experimental results also prove that our width label generation method can generate sufficiently realistic width labels for training our CNN-based method. If the training samples generated are not ideal enough, our CNN-based method cannot achieve such width estimation accuracy in the condition of cross-datasets.

Table 1. Results on REVIEW dataset

Method	HRIS		CLRIS		VDIS	
	SR (%)	σ_E	SR (%)	σ_E	SR (%)	σ_E
HHFW [2]	88.3	0.926	0	–	78.4	0.879
1D Gaussian [5]	99.6	0.896	98.6	4.137	99.9	2.11
2D Gaussian [6]	98.9	0.703	26.7	6.019	77.2	1.328
ESP [7]	99.7	0.42	93	1.469	99.6	**0.766**
Graph-based [8]	100	0.567	94.1	1.78	96	1.43
3D model [10]	99.4	0.65	98	1.56	97.8	1.14
Ours	**100**	**0.41**	**100**	**1.33**	**100**	1.41

In fact, the advantage of the CNN-based method lies not only in its estimation accuracy, but also in inference speed. Due to the complex image processing, existing automatic width estimation methods may take tens of seconds to process an image. While the CNN-based method only needs 30 ms (on an NVIDIA Titan XP GPU) to process an image with a resolution of 512×512, which can even achieve real-time performance.

4.2 Coronary Artery Width Estimation

Since there is no public dataset for coronary artery, no method can report its performance on this task, thus we cannot compare our method with other methods. However, as mentioned in dataset section, we use a coronary artery segmentation dataset to generate the training data and test data, thus we can run ablations to validate whether the idea of divide-and-conquer proposed in our CNN-based method can help obtain better vessel width estimation results.

For comparison, we respectively remove each branch of our CNN-based method to form two methods without the divide-and-conquer idea: (1) Regression Only: After removing the classification branch, the regression branch directly regresses the vessel width on full width range using a single regressor (instead of N regressors). (2) Classification Only: After removing the regression branch, we discretize the width values into 30 categories (1 to 30 pixels) and use the classification branch to classify the width value of all pixels.

Implementation Details: The input size of CNN-based method is 512×512. The coronary artery width ranges from 0 to 30 pixels. We set the sub-range to be 3, so there are 10 sub-ranges in all. We use an initial learning rate of 0.001, and the initial learning rate is multiplied by 0.8 every 1000 steps to avoid overfitting. Training takes about 2.5 h on an NVIDIA Titan XP for 200 epochs. Other details are the same as the experiments of retinal vessels.

Metric: Since the regression way can guarantee a 100% success rate, we only report the σ_E as the evaluation metric. Since the algorithm is expected to perform well over all widths, we will report the σ_E over different width ranges.

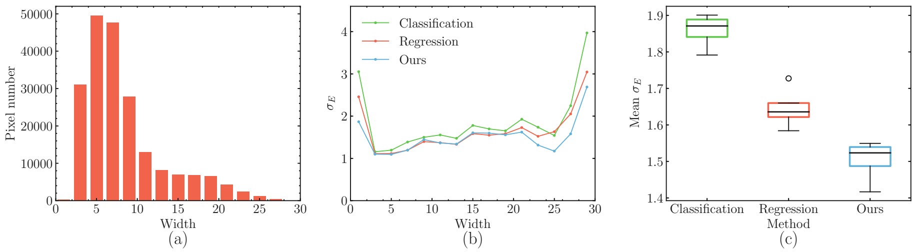

Fig. 4. Results: (a) Width distribution of samples. (b) The performance of three models at different width sub-range. (c) The box diagram of mean σ_E of three models

Specifically, we divide the range of 0 to 30 into 15 sub-ranges, and report the σ_E on all sub-ranges.

Experimental Results: The width distribution of our dataset is statistically analyzed in Fig. 4(a). It's clear that the width distribution is imbalanced. As shown in Fig. 4(b), this imbalance leads the width estimation algorithms to pay more attention to the sub-ranges with more samples. No matter the classification only or regression only, their performance on the thin vessels with more samples are significantly better than those on the thick vessels with fewer samples. However, after introducing the idea of divide-and-conquer, our proposed method maintains the performance on thin vessels, and significantly improves the performance on thick vessels, effectively alleviating the problem of sample imbalance. We also calculate the mean σ_E under different width ranges in multiple trials and draw a box diagram. As shown in Fig. 4(c), our method is significantly better than the comparison methods.

5 Conclusion

This paper proposes a CNN-based method for vessel width estimation, which is a brand new idea compared with the existing methods. In order to solve the most important challenge (lack of training data) when using CNN-based method, a method which can generate width labels using segmentation labels is also proposed. In order to solve the inevitable sample imbalance in the generated width labels, the idea of divide-and-conquer is introduced into our CNN-based method. In the experiments, we apply our method to retinal vessels, indicating that our method can achieve the state-of-the-art performance with less inference time. In addition, we apply our method to coronary arteries, indicating that the proposed divide-and-conquer method can alleviate the sample imbalance.

Acknowledgments. This work was supported in part by the National Natural Science Foundation of China under Grant 62073325, Grant 62003343, Grant U1913601, and Grant U20A20224; in part by the National Key Research and Development Program of China under Grant 2019YFB1311700; in part by the Youth Innovation Promotion Association of CAS under Grant 2020140; and in part by the Strategic Priority Research Program of CAS under Grant XDB32040000.

References

1. Klein, R., Klein, B.E., Moss, S.E.: The relation of systemic hypertension to changes in the retinal vasculature: the Beaver Dam Eye Study. Trans. Am. Ophthalmol. Soc. **95**, 329–350 (1997)
2. Brinchmann-Hansen, O., Heier, H.: Theoretical relations between light streak characteristics and optical properties of retinal vessels. Acta Ophthalmol. **64**, 33–37 (1986)
3. Rezaeian, M., Butlin, M., Golzan, S.M., Graham, S.L., Avolio, A.P.: A novel method for retinal vessel segmentation and diameter measurement using high speed video. In: 41st Annual International Conference of the IEEE Engineering in Medicine and Biology Society (EMBC), pp. 2781–2784 (2019)
4. Sun, G., Liu, X., Wang, S., Gao, L., Liu, M.: Width measurement for pathological vessels in retinal images using centerline correction and k-means clustering. Measurement **139**, 185–195 (2019)
5. Zhou, L., Rzeszotarski, M.S., Singerman, L.J., Chokreff, J.M.: The detection and quantification of retinopathy using digital angiograms. IEEE Trans. Med. Imaging **13**(4), 619–626 (1994)
6. Lowell, J., Hunter, A., Steel, D., Basu, A., Ryder, R., Kennedy, R.L.: Measurement of retinal vessel widths from fundus images based on 2-D modeling. IEEE Trans. Med. Imaging **23**(10), 1196–1204 (2004)
7. Al-Diri, B., Hunter, A., Steel, D.: An active contour model for segmenting and measuring retinal vessels. IEEE Trans. Med. Imaging **28**(9), 1488–1497 (2009)
8. Xu, X., et al.: Vessel boundary delineation on fundus images using graph-based approach. IEEE Trans. Med. Imaging **30**(6), 1184–1191 (2011)
9. Li, Q., You, J., Zhang, D.: Vessel segmentation and width estimation in retinal images using multiscale production of matched filter responses. Expert Syst. Appl. **39**(9), 7600–7610 (2012)
10. Aliahmad, B., Kumar, D.K.: Adaptive Higuchi's dimension-based retinal vessel diameter measurement. In: 38th Annual International Conference of the IEEE Engineering in Medicine and Biology Society (EMBC), pp. 1308–1311 (2016)
11. Huang, F., Dashtbozorg, B., Yeung, A.K.S., Zhang, J., Berendschot, T.T.J.M., ter Haar Romeny, B.M.: A comparative study towards the establishment of an automatic retinal vessel width measurement technique. In: Cardoso, M.J., et al. (eds.) FIFI/OMIA -2017. LNCS, vol. 10554, pp. 227–234. Springer, Cham (2017). https://doi.org/10.1007/978-3-319-67561-9_26
12. Zhang, T.Y., Suen, C.Y.: A fast parallel algorithm for thinning digital patterns. Commun. ACM **27**(3), 236–239 (1984)
13. Al-Diri, B., Hunter, A., Steel, D., Habib, M., Hudaib, T., Berry, S.: REVIEW - a reference data set for retinal vessel profiles. In: 30th Annual International Conference of the IEEE Engineering in Medicine and Biology Society (EMBC), pp. 2262–2265 (2008)
14. Li, W., Lu, J., Feng, J., Xu, C., Zhou, J., Tian, Q.: BridgeNet: a continuity-aware probabilistic network for age estimation. In: Proceedings of 2019 IEEE/CVF Conference on Computer Vision and Pattern Recognition (CVPR), pp. 1145–1154 (2019)
15. Chen, S., Zhang, C., Dong, M., Le, J., Rao, M.: Using ranking-CNN for age estimation. In: Proceedings of 30th IEEE/CVF Conference on Computer Vision and Pattern Recognition (CVPR), pp. 742–751 (2017)

16. Ronneberger, O., Fischer, P., Brox, T.: U-Net: convolutional networks for biomedical image segmentation. In: Navab, N., Hornegger, J., Wells, W.M., Frangi, A.F. (eds.) MICCAI 2015. LNCS, vol. 9351, pp. 234–241. Springer, Cham (2015). https://doi.org/10.1007/978-3-319-24574-4_28
17. Staal, J., Abramoff, M.D., Niemeijer, M., Viergever, M.A., van Ginneken, B.: Ridge-based vessel segmentation in color images of the retina. IEEE Trans. Med. Imaging **23**(4), 501–509 (2004)
18. Kingma, D.P., Ba, J.L.: Adam: a method for stochastic optimization. In: Proceedings on 3rd International Conference on Learning Representations (ICLR), pp. 1–15 (2015)